Nuclear magnetic resonance and molecular dynamics study of methanol up to the supercritical region

Nobuyoshi Asahi and Yoshio Nakamura

Citation: The Journal of Chemical Physics **109**, 9879 (1998); doi: 10.1063/1.477656
View online: http://dx.doi.org/10.1063/1.477656
View Table of Contents: http://scitation.aip.org/content/aip/journal/jcp/109/22?ver=pdfcov
Published by the AIP Publishing

Nuclear magnetic resonance and molecular dynamics study of methanol up to the supercritical region

Nobuyoshi Asahi and Yoshio Nakamura
Division of Chemistry, Graduate School of Science, Hokkaido University, Sapporo 060-0810, Japan

(Received 1 June 1998; accepted 1 September 1998)

Self-diffusion coefficients and chemical shifts of the methanol OH proton referred to the CH_3 proton have been measured in a wide temperature range from 289 to 580 K. The reduced densities ρ_r ($\rho_r=\rho/\rho_C$, $\rho_C=272$ kg m^{-3}) of methanol studied are 0.183, 0.256, 0.372, 0.622 and 1.008 in the supercritical condition. Molecular dynamics (MD) simulations have been performed in the same temperature and density range. The observed self-diffusion coefficients are in a good agreement with the Chapman-Enskog kinetic theory in the supercritical region. They are consistent with the MD simulation results over the whole range studied. MD calculations show that hydrogen-bonded clusters of methanol are chain like both at room temperature and in the supercritical state. The formation energy and entropy of hydrogen bonding were obtained from the temperature dependence of the OH chemical shifts for supercritical methanol. The thermodynamic model which takes account of cluster distribution provides the degree of hydrogen bonding in methanol. The number of hydrogen-bonded clusters decreases with increasing temperature and decreasing density. In the supercritical region, the calculated results for the cluster size distribution from the thermodynamic model are in a good agreement with the MD calculation. © *1998 American Institute of Physics.* [S0021-9606(98)50846-X]

I. INTRODUCTION

It is interesting to study the local structure and dynamics of liquid and supercritical methanol which is a self-associated liquid assigned to hydrogen bonding between OH oxygen and OH hydrogen. Hydrogen-bonded compounds such as water, methanol or acetic acid are known as playing an important role in natural phenomena and chemistry.[1] Methanol in the supercritical state, in particular, has provided a great interest for fundamental and engineering research fields.[2,3] Even in simple hydrogen-bonded liquids, however, unusual molecular interactions and specific molecular properties are remained to be elucidated in contrast to non-hydrogen-bonded liquids.

A great number of investigations have been made to reveal the thermodynamic, structural and dynamic properties of methanol, e.g., nuclear magnetic resonance (NMR) spectroscopy,[4–10] x-ray scattering,[11,12] neutron scattering,[13] Raman spectroscopy,[14,15] and computer simulation.[9,16–21] Jonas and Akai[5] investigated the self-diffusion coefficient of methanol-OD by NMR at temperatures from 223 to 323 K and pressures up to 5 kbar. They attributed to the decrease of the hydrogen bonding with increasing pressure that the observed change in the Stokes-Einstein coefficient from stick boundary condition to slip boundary condition. Karger *et al.*[6] studied methanol and methanol-OD between 150 and 450 K and at pressures up to 2.5 kbar. They showed that *A*-parameter in Chandler's rough hard sphere model decreases drastically with falling temperature. This can be ascribed not only to rotation-translation coupling but also to hydrogen bonding. Oldenziel and Trappeniers[7] reported the pressure dependence of NMR chemical shifts of methanol at room temperature. They found the chemical shifts increase with increasing pressure. These results reflect an increase in hydrogen-bonded methanol with increasing pressure. Shulman *et al.*[8] made a chemical shift study from 278.3 to 391.7 K and from 0.1 to 1 kbar. Based upon a monomer/tetramer model[22–24] they showed that the degree of association increases with decreasing temperature and with increasing pressure. Wallen *et al.*[9] investigated the temperature and pressure denpendence of the distribution of hydrogen-bonded clusters ranging from 297 to 413 K and up to 2.8 kbar in their NMR chemical shift and molecular dynamics (MD) study. Their MD results are coincident with the previous chemical shift study.[7,8] On the contrary, the hydrogen bond networks derived from a thermodynamic aggregation model[9,25] are not consistent with the results from their MD and chemical shift study. Recently, Hoffmann and Conradi[10] reported the chemical shifts of both methanol and ethanol in the temperature range up to 723 K and at pressures up to 350 bar. They concluded that methanol has hydrogen bonding at gaslike densities in the supercritical region even at 723 K. They showed by use of a simple two state model that the enthalpy of hydrogen bond formation in methanol is 12.8 kJ mol^{-1}.

NMR provides a best technique to investigate the local electronic environment due to both the molecular structure and molecular motion.[4,26–28] Molecular dynamics simulation also provides a useful tool to deduce the molecular structure and molecular motion of fluids. The potentials used are regarded reasonable, if the results of MD simulation can reproduce static and dynamic properties of the real systems such as radial distribution functions and transport coefficients. As far as we know, no investigations have so far been reported with regard to self-diffusion coefficients and MD simulations

of methanol up to the supercritical region. The purpose of the present study is to elucidate the dynamic properties and hydrogen bonding in methanol at molecular level for a wide range of temperature and density including the supercritical region.

II. EXPERIMENT

All NMR measurements were made with a Bruker CXP NMR spectrometer which has a modified JEOL wide bore iron magnet with an external lock system operating at 38.3 MHz. The apparatus including the high temperature-high pressure probe has been described elsewhere.[4,26,27] Methanol (Wako Pure Chemical Industries) of spectroscopic grade was dried at least for a week by using molecular sieves, distilled under vacuum, and then sealed in a Pyrex glass cell after sufficient degassing. Methanol sealed in the NMR cell was heated and pressurized with its own vapor. The sample cell was pressurized externally up to 160 bar by helium gas to suppress the internal vapor pressure of methanol. Five samples with the reduced densities (referred to the critical density, 272 kg m^{-3} (Refs. 29,30) of 0.183, 0.256, 0.372 and 1.008 in the supercritical condition were used.

A. Self-diffusion coefficient

The self-diffusion coefficients were measured by the Carr-Purcell-Meiboom-Gill (CPMG) pulse sequence.[31,32] It is known that this technique has no advantage on normal liquid in contrast to the spin-echo method.[33] However, in a previous study,[26] we have shown that the CPMG method is the best for measurements of supercritical fluids which exhibit an extreme motional narrowing in high pressure-high temperature conditions. In the CPMG method, the relation for the self-diffusion coefficient D, the echo intensity A_{on} with a magnetic field gradient and the echo intensity A_{off} without the gradient is given by

$$\ln \frac{A_{\mathrm{on}}(t)}{A_{\mathrm{off}}(t)} = -\frac{1}{3} D \gamma^2 G^2 \tau^2 t, \tag{1}$$

where γ is the gyromagnetic ratio of proton, and 2τ is the interval between two π-pulses. The field gradient G was generated by a pair of Helmholtz coils attached to the cooling jacket which covered the vessel and its magnitudes was determined from the analysis of echo-forms. There are two types of errors in determining the self-diffusion coefficients. The one is from the error in the field gradient calibration and the other is from the echo intensity error due to low S/N ratio. The estimated error from these sources was $\pm 4\%$. The present experimental result for pure methanol at 288 K, $D = 1.93 \times 10^{-9} \mathrm{m^2\ s^{-1}}$, is in a good agreement with the value from an isotopic tracer diffusion study,[34] $D = 1.91 \times 10^{-9}\ \mathrm{m^2\ s^{-1}}$.

B. Chemical shift

Chemical shifts were measured by Fourier transformation after a FID acquisition. The spectroscopic resolution was 1 Hz (0.025 ppm). Although the nuclear shielding constant for a methanol molecule consists of various contributions,[35–37] the effect of hydrogen bonding interaction is much larger than any other contributions. As the CH_3 and non-hydrogen-bonded OH protons have a similar local magnetic environment, the temperature and density dependences of the respective chemical shifts are almost the same. We have thus determined the chemical shifts of the OH proton referred to the CH_3 proton.

III. MOLECULAR DYNAMICS METHOD

Molecular dynamics simulation was performed with the MDMPOL program coded by Smith and Fincham,[38] in which a molecule was kept rigid and the translational motion for the center-of-mass was solved by a leapfrog algorithm. The angular motion was treated by using a leapfrog-quaternion algorithm. Jorgensen's transferable intermolecular potential (TIP) model[18] was used for the intermolecular interaction of methanol molecules. The Lennard-Jones and Coulomb site-site terms are used in the potential which consists of three sites, CH_3 group, O atom and hydroxyl H atom. The form of this 12-6-1 potential is

$$U_{\alpha\beta} = 4\varepsilon_{\alpha\beta}\left(\left(\frac{\sigma_{\alpha\beta}}{r_{\alpha\beta}}\right)^{12} - \left(\frac{\sigma_{\alpha\beta}}{r_{\alpha\beta}}\right)^{6}\right) + \frac{q_\alpha q_\beta}{4\pi\varepsilon_0 r_{\alpha\beta}}, \tag{2}$$

where α and β are unlike molecular sites respectively, and $r_{\alpha\beta}$ is the site-site separation. The Lennard-Jones parameters $\sigma_{\alpha\beta}$ and $\varepsilon_{\alpha\beta}$ between different sites are calculated with the following Lorentz-Berthelot mixing rules

$$\sigma_{\alpha\beta} = (\sigma_{\alpha\alpha} + \sigma_{\beta\beta})/2, \quad \varepsilon_{\alpha\beta} = \sqrt{\varepsilon_{\alpha\alpha}\varepsilon_{\beta\beta}}. \tag{3}$$

The potential parameters used and geometries are the same as those reported previously.[18] The electrostatic potential was treated by the Ewald summation method. Molar volumes are chosen as reproducing the experimental molar volumes.[30] The simulations were carried out for a microcanonical system of 256 molecules in a cubic unit cell, using the periodic boundary condition. The time step was 2.5 fs and the configurations were accumulated every 50 time steps for successive 4000 to 9000 steps after a 3000 step equilibration. The four calculations were performed at a given temperature and density with a different set of initial random numbers. We have also made MD simulations with and without the fractional charge (FC) in order to examine the hydrogen bond or polarity effects.

The unlike site-site potential parameters were not treated with OPLS combining rules[18] in the present study. It is noted that the results of MD simulation[20] with the present model potential and Lorentz-Berthelot mixing rules are in a good agreement with the experimental results of partial pair radial distribution functions from x-ray diffraction[12] and self-diffusion coefficients[6,39] for liquid methanol at room temperature.

IV. RESULTS AND DISCUSSION

A. Self-diffusion coefficient

The experimental and simulated self-diffusion coefficients of methanol both in the liquid and supercritical state are given in Tables I–IV. Figure 1 also shows graphically the self-diffusion coefficient of methanol as a function of tem-

TABLE I. Experimental results of the self-diffusion coefficient of liquid methanol.

T/K	$D/10^{-9}$ m^2 s^{-1}
288	1.93
340	4.52
367	6.57
399	9.99
432	15.1
452	18.6
469	24.5
475	25.2
490	34.8

perature. The diffusion coefficient of liquid methanol shows little density dependence under vapor-liquid saturation, but a large density dependence under the supercritical condition. From a little below the critical point the self-diffusion coefficient increases rapidly as temperature increases, corresponding to a rapid change in liquid density. The present results of self-diffusivities of methanol are similar to those of benzene in our previous study.[26]

The temperature and density dependencies of the self-diffusion coefficient of supercritical methanol can be discussed on the basis of the Chapman-Enskog equation derived for Lennard-Jones fluids.[40] The equation for the first approximation is given by

$$D=\frac{3(\pi k_{\mathrm{B}}T/m)^{1/2}}{8\pi n\sigma^2\Omega^{(1,1)*}(T^*)}, \tag{4}$$

where m and n are respectively the mass and the number density of the molecules studied. k_{B} is the Boltzmann constant and T^* is the temperature expressed as $T^*=k_{\mathrm{B}}T/\varepsilon$. ε and σ are the parameters appearing in the Lennard-Jones (LJ) potential equation. $\varepsilon/k_{\mathrm{B}}$ and σ for methanol are respectively 507 K and 3.585 nm.[40] The collision integrals $\Omega^{(1,1)*}(T^*)$ calculated for the LJ potential are taken from the table of the Ref. 41. The calculated results are shown in Fig. 1 and compared with the experimental results. In this kinetic model, it is assumed that the molecular shape is spherical and the collision between molecules is only binary collision in a dilute gas. In spite of these assumptions, the calculated values from Eq. (4) are in a good agreement with the experimental values in the supercritical region. The Chapman-Enskog equation, however, cannot give the self-diffusion coefficient in the liquid state due to the assumption of binary collision.

TABLE II. Experimental results of the self-diffusion coefficient for methanol near and above the critical temperature (513 K).

ρ_{r}	T/K	$D/10^{-9}$ m^2 s^{-1}
0.183	509	408
	526	438
	561	502
	571	423
	580	453
0.372	506	192
	515	201
	524	204
	538	210
	561	225
	571	229
0.622	511	114
	531	125
	543	129
	553	136
	566	134
	574	136
1.008	513	69.9
	535	83.6
	557	88.4
	580	88.9

TABLE III. Simulation results of self-diffusion coefficient and average potential energy of liquid methanol (with FC).

T/K	$D/10^{-9}$ m^2 s^{-1}	$-U$/kJ mol^{-1}
293±11	1.76±0.31	36.96±0.33
340±11	4.00±0.74	33.88±0.36
400±11	10.7±1.4	29.61±0.09
470±11	22.3±2.5	23.80±0.40

There are two ways to calculate the self-diffusion coefficient from MD simulations. The one is from integration of velocity autocorrelation function, and the other is from the mean square displacement of molecules via Einstein relation. In this study, the latter was used. The expression is

$$D=\lim_{t\to\infty}\frac{1}{6}\frac{\mathrm{d}}{\mathrm{d}t}\langle|\mathbf{r}_i(t)-\mathbf{r}_i(0)|^2\rangle, \tag{5}$$

where $\mathbf{r}_i$ is the positional vector, and the bracket $\langle\rangle$ represents the average over 256 molecules. The calculated results both with and without FC are also shown in Fig. 1. The self-diffusion coefficients from the simulations with FC are in an excellent agreement with the experimental values in the whole temperature and density range studied, while the results without FC are in poor agreement. The results with FC clearly show that the retarding effect due to attractive potentials on translational diffusion is important in the liquid state.[6] The calculated results without FC are, however, closer to the observed values only at higher temperatures as shown in Fig. 1. In the supercritical region, the results with and without FC are almost identical and the extra attractive interaction gives no retarding effect. This is the reason why the Chapman-Enskog approach with the LJ potential is in a good agreement with experiments in the supercritical region.

TABLE IV. Simulation results of self-diffusion coefficient and average potential energy of supercritical methanol (with FC).

ρ_{r}	T/K	$D/10^{-9}$ m^2 s^{-1}	$-U$/kJ mol^{-1}
0.183	525±17	439±19	2.86±0.16
	575±14	474±60	3.55±0.04
0.372	525±19	212±50	5.54±0.15
	575±17	253±15	7.01±0.12
0.622	525±19	126±22	8.56±0.55
	575±17	148±11	10.61±0.24
1.008	525±17	81.0±7.3	12.35±0.29
	575±22	93.2±2.1	13.98±0.32

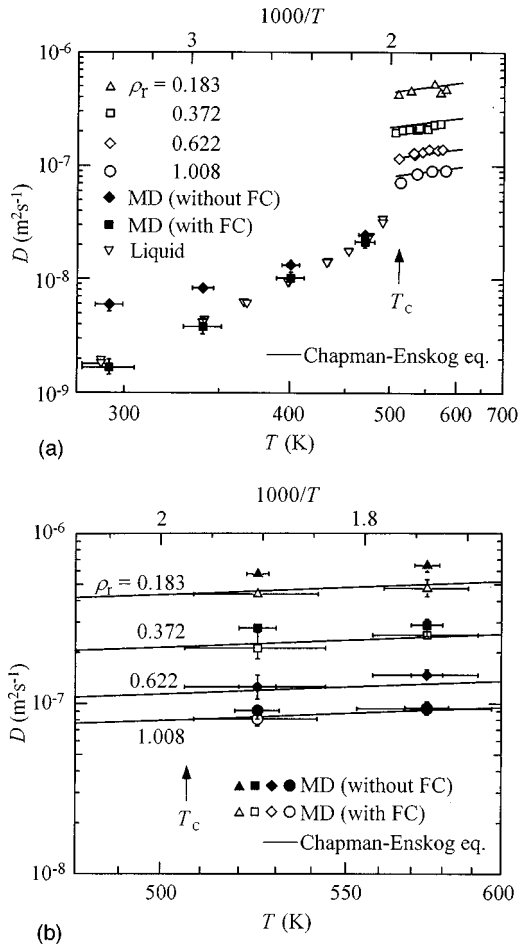

FIG. 1. (a) Experimental and simulated results of the self-diffusion coefficient of methanol as a function of temperature. The results of MD simulation are omitted in the supercritical region. The observed diffusion coefficients below the critical temperature T_C are for liquid under the liquid-vapor coexistence. The solid lines are the calculated results from the Chapman-Enskog theory. (b) Enlargement of (a) in the supercritical region. The solid lines are the calculated values from the Chapman-Enskog equation. Open and filled marks denote the diffusion coefficients from MD simulations with and without FC, respectively. The reduced densities in each simulation are 0.183 (△), 0.372 (□), 0.622 (◇), and 1.008 (○). The experimental data are omitted.

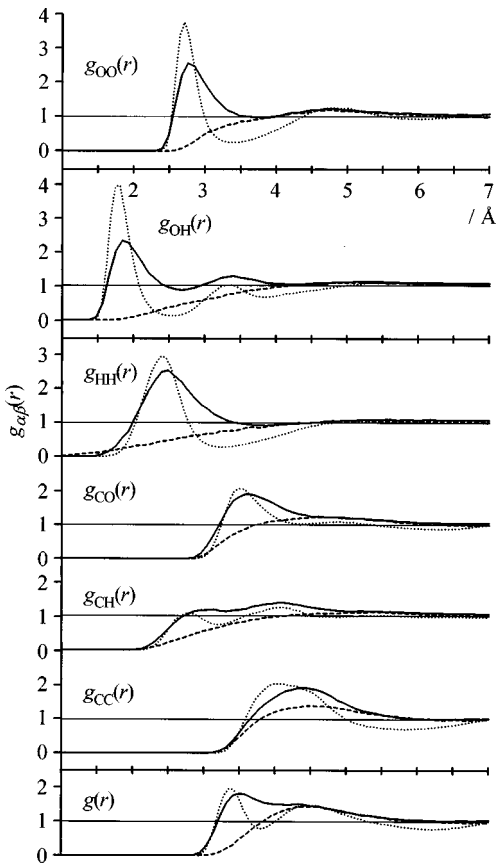

FIG. 2. Partial pair correlation function obtained from MD simulations for supercritical methanol at 525 K and $\rho_r = 1.008$. The solid lines are the calculated results with FC and the broken lines are those without FC. The pair correlation functions for liquid methanol at 293 K are also shown by dotted lines. $g(r)$ is the correlation function for the center of mass of the respective molecules.

The self-diffusion coefficients from the present MD simulation with the potential given by Eq. (2) are in an excellent agreement with experiments both in the liquid and supercritical states. Thus, we will examine further information on the structure of liquid and supercritical methanol from MD simulations using the same potential model.

B. Pair correlation function

Here, we discuss the static structures of methanol from the results of MD simulation. It is very useful to calculate the atom-atom pair correlation function $g_{\alpha\beta}(r)$ in order to study the local structure of liquids. The pair correlation functions are calculated from the following equation

$$g_{\alpha\beta}(r) = \left\langle \frac{n_\beta(r_{\alpha\beta}, r_{\alpha\beta}+\mathrm{d}r_{\alpha\beta})}{4\pi\rho r_{\alpha\beta}^2 \mathrm{d}r_{\alpha\beta}} \right\rangle, \tag{6}$$

where α and β are atoms on different molecules. ρ is the number density of methanol molecules, $r_{\alpha\beta}$ is the atom-atom separation, and n_β is the number of β atoms in the volume element between $r_{\alpha\beta}$ and $r_{\alpha\beta}+\mathrm{d}r_{\alpha\beta}$. The calculated results for six correlation functions are given in Fig. 2. The shapes of these functions are similar to those reported by Jorgensen *et al.*[16–18] and Haughney *et al.*[20] from MD simulations. The maximum and minimum positions are in a close agreement with their values. At room temperature the first sharp peaks in the pair correlation functions, in particular, in $g_{OO}(r)$, $g_{OH}(r)$, and $g_{HH}(r)$, are attributed to the short range structure due to hydrogen bonding. In every correlation function, the first peaks are broader at 525 K than at 293 K, and the peak positions shift to a larger distance. Thus, the hydrogen bonding of methanol in the supercritical region (525 K) is weaker than that at room temperature. The difference between the pair correlations simulated with and without FC demonstrates that the hydrogen bond structure exists even in the supercritical region. The second peak in the $g_{OH}(r)$ function remains at 3.4 Å in the supercritical state. This suggests that hydrogen-bonded clusters are not only in the dimer state but also in the chain-like trimer state. The O-O and O-H coordination numbers are calculated by integrating the respective correlation functions up to the first minimum. The coordination numbers are about 2 and 1 for the O-O corre-

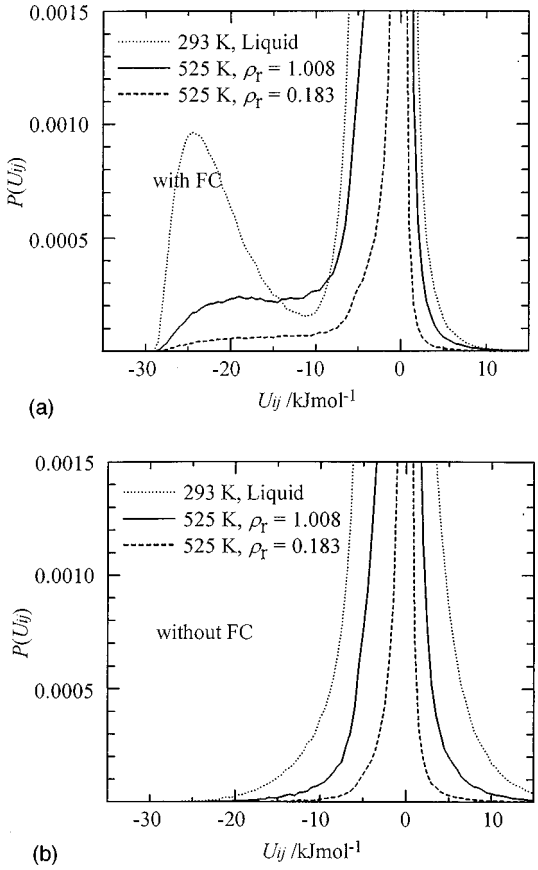

FIG. 3. (a) Distributions of the pair interaction energy from MD simulations with FC. The solid line is the distribution at 525 K and $\rho_r = 1.008$. The broken line represents distributions for supercritical methanol at 525 K and $\rho_r = 0.183$. Distribution for liquid methanol is shown by dotted line. (b) Distributions from MD simulations without FC. The symbols are the same as in (a).

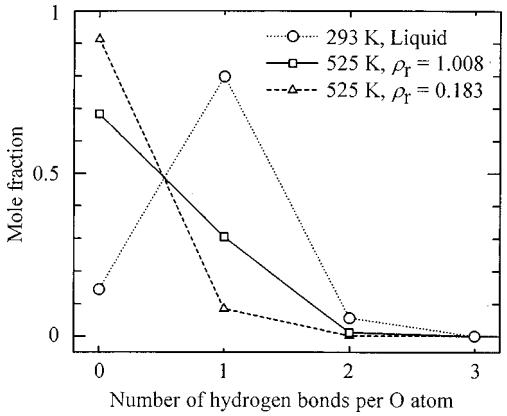

FIG. 4. Mole fractions of the hydrogen-bonded O atoms as a function of number of hydrogen bonds per O atom in liquid (293 K) and supercritical (525 K) methanol.

lation function at 293 and 525 K, respectively. They are respectively about 1 and 0.5 for the O-H correlation function at 293 and 525 K. The average number of the nearest hydrogen-bonded neighbors at 525 K is a half of that at 293 K. Therefore, we examine next the structure and aggregations of hydrogen-bonded clusters in methanol at molecular levels.

C. Hydrogen bonding

The pair interaction energy distributions $P(U_{ij})$ calculated with and without FC are shown in Fig. 3 as a function of pair interaction energy U_{ij}. A pair of methanol molecules show a large negative energy shift at the separation corresponding to hydrogen bonding than at any other separations. There is a peak at about -25 kJ mol^{-1} in pair energy with FC due to hydrogen bonding and no such peak is observed without FC. Similar shapes of $P(U_{ij})$ have been reported for other hydrogen-bonded liquids.[16–20,42–44] Very large $P(U_{ij})$ around 0 energy represents a contribution of a large number of methanol molecule pairs at large distances. The peak height at $U_{ij} = -25$ kJ mol^{-1} decreases with increasing temperature and decreasing density, while the peak height at $U_{ij} = 0$ increases. This change in peak heights shows that the number of hydrogen-bonded clusters decreases with increasing temperature and decreasing density. The hydrogen bonding, however, is still observed even at 525 K and $\rho_r = 0.183$ as a shoulder around -20 kJ mol^{-1}, as shown in Fig. 3(a).

As the first sharp peak in the pair correlation function $g_{OH}(r)$ represents the strong short range order of hydrogen bonding, the first minimum may be considered as a limit of separation between the O atom and H atom to form a hydrogen bond. In other words, if the distance between intermolecular O and H atoms lies within the first minimum, ''hydrogen bond'' is formed between the two molecules. Alternatively, a pair of methanol molecules are regarded to be ''hydrogen-bonded'' when the potential energy is smaller than the minimum value at $U_{ij} = -11$kJ mol^{-1}.

Thus, there are two criteria for hydrogen bond formation; the geometric one from intermolecular atom-atom separation or the energetic one from pair energy distribution. Each criterion, geometric[20,45] or energetic one,[16–18,44] has been applied to hydrogen-bonded liquids. These definitions, however, are somewhat arbitrary because of the continuous nature both in the configuration and the energy distribution. A combination of the geometric and energetic criteria should be used at the same time, if the two definitions are not consistent with each other. In the Monte Carlo study, Kalinichev *et al.*[43] have discussed the criteria for hydrogen bonding in water at 773 K up to 10000 MPa. They have shown that the energetic definition is more effective than the geometric one, and at high pressures, in particular, a combination of the both definitions may be preferable. In the present study, therefore, we adopt both the geometric and energetic criteria.

D. Configuration of hydrogen bonding

An O atom can form two hydrogen bonds at most due to two lone pairs per atom. Figure 4 shows the mole fraction of hydrogen-bonded O atoms as a function of number of hydrogen bonds per O atom. The mole fraction of doubly hydrogen-bonded O atoms is small. This means that few clusters of methanol molecules have Y junctions or doubly hydrogen-bonded O atoms. In other words the dominant shape of clusters is chain-like. As shown in Fig. 4, the ratio of methanol monomers increases with increasing tempera-

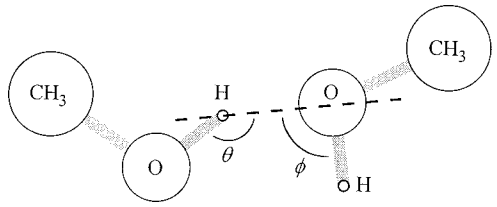

FIG. 5. Definition of the hydrogen bond angles for a pair of methanol molecules.

ture and decreasing density. The distribution of hydrogen-bonded clusters will be treated more quantitatively in the Sec. IV F.

The hydrogen bond angles expressed as θ and ϕ are defined in Fig. 5. The cosine distributions of the two angles are shown in Fig. 6. The distribution of $\cos\theta$ has a maximum at -1, that is, $\theta=180°$. The distribution of $\cos\phi$ has a broad maximum around -0.5, that is, $\phi=120°$. A similar result has been obtained for liquid hydrogen fluoride,[44] but somewhat different results have been given in Monte Carlo studies[16–19] for liquid methanol. The angular distributions become broad at higher temperatures and lower densities. Although no directionality of the O atom is considered in the model potential, the present results are in a good agreement with the results of the *ab initio* calculation[19] for a linear dimer.

E. Chemical shift results

Figure 7 shows the chemical shifts of the OH proton referred to the CH_3 proton for liquid and supercritical methanol. The isochoric data of Wallen *et al.*[9] up to 413 K are also shown. In the present study methanol is under the vapor-liquid equilibrium below the critical temperature T_C. The chemical shifts decrease with increasing temperature and, in particular, a rapid decrease is found a little below the critical temperature. In the supercritical region, the chemical shifts show a relatively small temperature dependence and a large density dependence. These changes in the chemical shifts of the OH proton can be interpreted in terms of change in the hydrogen bonding in methanol. The formation of hydrogen bonding between the OH groups of unlike molecules causes a higher frequency shift due to lowering of the electron density around the proton. Thus, the present results of proton chemical shifts show that the number of hydrogen bonds decrease with increasing temperature and decreasing density. These results are consistent with those of the previous studies for methanol[7–10] and also in agreement with those of pair correlation functions and pair interaction energies from MD simulations given in the previous sections.

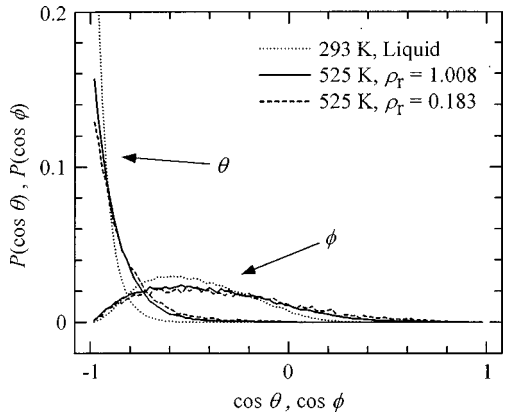

FIG. 6. Cosine angle distribution of the hydrogen bonds in liquid and supercritical methanol. The solid and broken lines are cosine angle distributions in the supercritical region, $\rho_r=1.008$ and $\rho_r=0.183$ at 525 K, respectively. The dotted line is the cosine angle distribution in the liquid state at 293 K.

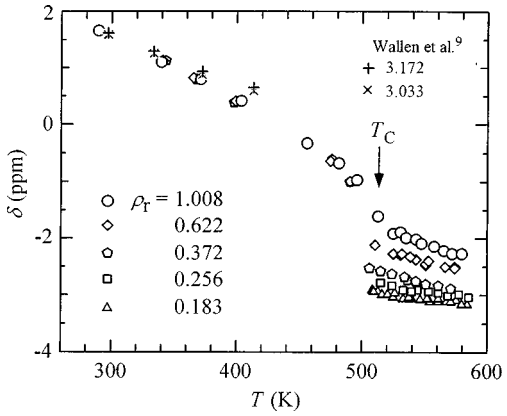

FIG. 7. Chemical shifts of the OH proton referred to the CH_3 proton as a function of temperature. Methanol is under the gas-liquid coexistence below the critical temperature. (+) and (×) represent the isochoric data of Wallen *et al.* (Ref. 9).

F. Hydrogen-bonded cluster distribution

The measured chemical shift is a weight-average of all species shifts, since the lifetime of a hydrogen bonding is much shorter than the NMR observation time. We assume here that the observed chemical shifts are due to two species, i.e., the hydrogen-bonded OH proton and the non-hydrogen-bonded OH proton. If we assume the additivity, the observed chemical shift δ is expressed as[46]

$$\delta=x_{\text{N-HB}}\delta_{\text{N-HB}}+(1-x_{\text{N-HB}})\delta_{\text{HB}}, \tag{7}$$

where $\delta_{\text{N-HB}}$ is the contribution of non-hydrogen-bonded protons, and δ_{HB} is the contribution of hydrogen-bonded protons. $x_{\text{N-HB}}$ is the mole fraction of non-hydrogen-bonded protons. $\delta_{\text{N-HB}}$ needs to be known in order to determine the mole fraction of the hydrogen-bonded protons. It has been shown that the chemical shift of non-hydrogen-bonded protons referred to TMS is 0.8 ppm for liquid methanol from an infinite dilution method in the monomer/tetramer model.[22–24] In the present study, however, the chemical shifts are referred

TABLE V. Refitted results to the equilibrium model for the liquid methanol data of Wallen *et al.* (Ref. 9). Figures in parentheses represent their results.

ρ_r	ΔS/J mol^{-1} K^{-1}	ΔE/kJ mol^{-1}	δ_{HB}
3.033	−25.4	−17.6	2.26
	(−27.26)	(−18.92)	—
3.172	−24.7	−17.6	2.26
	(−24.89)	(−17.84)	—

TABLE VI. Regression results for supercritical methanol at constant density.

ρ_r	ΔS/J mol^{-1} K^{-1}	ΔE/kJ mol^{-1}
0.183	−56.9±4.4	−19.4±2.3
0.256	−49.3±4.2	−16.9±2.1
0.372	−61.9±3.2	−25.3±1.6
0.622	−45.5±3.7	−19.1±1.7
1.008	−49.2±2.9	−22.9±1.3

TABLE VII. Mole fractions of the non-hydrogen-bonded OH protons, $x_{\text{N-HB}}$, in supercritical methanol.

ρ_r	525 K	550 K	575 K
0.183	0.922	0.935	0.944
0.256	0.897	0.911	0.922
0.372	0.858	0.885	0.905
0.622	0.792	0.818	0.840
1.008	0.726	0.763	0.793

to the CH_3 proton, and we have used the value of $\delta_{\text{N-HB}} = -3.45$ ppm obtained in our previous study.[4] This value is consistent with the results of methanol gas-phase studies, −3.47 ppm by Clague *et al.*[47] and −3.40 ppm by Hoffmann and Conradi.[10]

We use here a thermodynamic model (see Appendix) which involves cluster distributions based on the value of $\delta_{\text{N-HB}}$ and Eq. (7). We assume that methanol clusters are ''chain'' with no branches, and all of the hydrogen bonds are identical in a cluster in which the chemical potential of a methanol molecule is equal. These assumptions are substantiated by the previous sections. We can determine the parameters δ_{HB}, x_1, x_n, and $x_{\text{N-HB}}$, by a three-parameter fitting using Eqs. (7), (A4), (A5), and (A6) and the expression $\Delta F = \Delta E - T\Delta S$. Since our data of δ, however, show a small temperature dependence $((\partial\delta/\partial T)_\rho)$ in the supercritical region, they are not sufficient for three-parameter regressions. We have therefore performed first a three-parameter regression for the isochoric data of Wallen *et al.*[9] for liquid methanol. The results are given in Table V. We have obtained $\delta_{\text{HB}} = 2.26$ ppm referred to the CH_3 proton. The refitted values of the entropy ΔS and energy ΔE of hydrogen bond formation are somewhat different from their values.[9]

We have then made a two-parameter fitting with the chemical shifts in the supercritical state using the value of $\delta_{\text{HB}} = 2.26$ ppm. The results are summarized in Table VI. From Eq. (A5), ΔS, and ΔE, we have calculated the mole fraction and the size of hydrogen-bonded clusters in methanol. Figure 8 shows the mole fraction of the *n*-mer clusters as a function of cluster size from MD and the thermodynamic model. The calculated results from the thermodynamic model are in an excellent agreement with those of MD. It is clear that the distributions depend both on temperature and density. As shown in Fig. 8, the cluster size distributions shift toward smaller clusters at higher temperatures. As the density decreases, the distributions become narrower. The degree of hydrogen bonding decreases with increasing temperature and decreasing density. In Table VII are given the mole fractions of non-hydrogen-bonded protons $x_{\text{N-HB}}$ for various temperatures and densities in the supercritical state. As expected from the chemical shift data, the change in hydrogen bond number with density is larger than that with temperature in the range of our study. The existence of hydrogen-bonded cluster at gaslike densities is in agreement with the previous results of Hoffmann and Conradi.[10] They reported, however, a somewhat smaller value (−12.8 kJ mol^{-1}) for the energy of hydrogen bonding formation than the present value of −20 kJ mol^{-1}. This is because they used a simple two state model assuming noninteracting hydrogen bonds.

The mole fractions of non-hydrogen-bonded protons $x_{\text{N-HB}}$ at higher liquid densities due to Wallen *et al.*[9] are recalculated by using the parameters given in Table V. In Table VIII, our refitted results show that values of $x_{\text{N-HB}}$

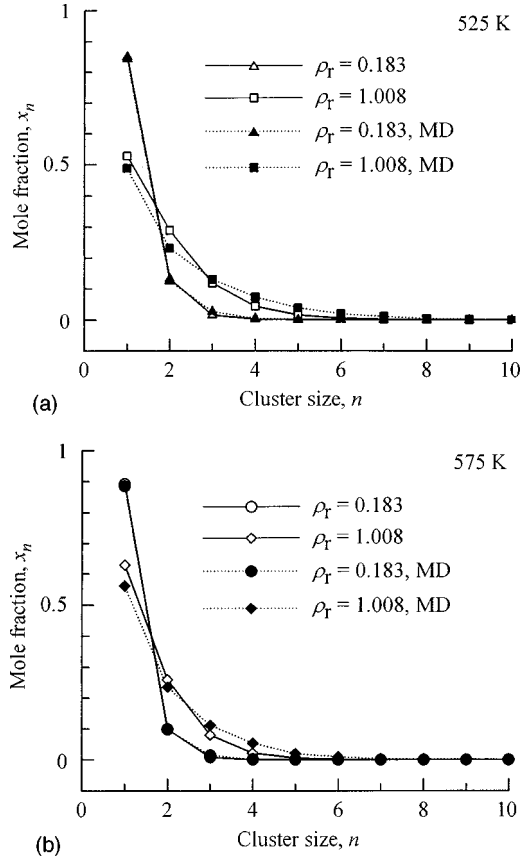

FIG. 8. (a) *n*-mer mole fractions through the monomer as a function of cluster size *n* at 525 K. The open and filled marks are, respectively, the calculated results from the thermodynamic model and those from MD simulations. (b) *n*-mer mole fractions through the monomer at 575 K.

TABLE VIII. Mole fractions of the non-hydrogen-bonded OH protons, $x_{\text{N-HB}}$, in liquid methanol from the data of Wallen *et al.* (Ref. 9). Figures in parentheses represent their calculated results.

ρ_r	297.3 K	413.2 K
3.033	0.123	0.298
	(0.106)	(0.279)
3.172	0.118	0.287
	(0.114)	(0.282)

decrease remarkably with increasing density, that is, the hydrogen bonding increases as the density increases in contrast to their results.[9] This discrepancy may be attributed to their neglect of both the temperature and density dependencies of $\delta_{\text{N-HB}}$ referred to TMS.

V. CONCLUDING REMARKS

The self-diffusion coefficients and chemical shifts of the OH proton referred to the CH_3 proton in methanol have been measured in a wide temperature range including the supercritical region. MD simulations have also been performed in *NVE* ensembles with Jorgensen's TIP model. The observed results of self-diffusion coefficients in the supercritical region are in a good agreement with those calculated from the Chapman-Enskog theory. The self-diffusion coefficients are also in an excellent agreement with MD results over the whole temperature and density range of this study. The results of self-diffusion coefficient with and without fractional charges show that the retarding effect on translational motion is important only in the liquid state. MD simulations also show that methanol clusters are chain-like both at room temperature and in the supercritical state. The number of hydrogen-bonded clusters has been calculated from the chemical shift data by means of the thermodynamic aggregation model which considers the cluster distributions. In the supercritical region, the results for cluster distribution from the thermodynamic model are in a good agreement with the results of MD calculation.

ACKNOWLEDGMENTS

The authors wish to thank Professor S. Ikawa for inspiring discussions about MD simulations. They also acknowledge Dr. T. Kamiyama for useful discussions in MD programs, and Mr. E. Yamada for helpful advices and encouragement during the course of this study.

APPENDIX: THERMODYNAMIC AGGREGATION MODEL

The distribution of the hydrogen-bonded clusters in methanol has been discussed in terms of the thermodynamic aggregation model.[9,25] As various sizes of hydrogen-bonded clusters are in equilibrium, the chemical potential μ of every methanol molecule in the clusters is the same and expressed as follows:

$$\mu=\mu_1^0+kT\log x_1$$
$$=\mu_2^0+\frac{kT}{2}\log\frac{x_2}{2}=\cdots=\mu_n^0+\frac{kT}{n}\log\frac{x_n}{n}, \tag{A1}$$

where μ_1^0, μ_2^0, μ_n^0 are the chemical potential of the monomer, dimer and *n*-mer, and x_1, x_2, x_n are the mole fraction of monomer, dimer and *n*-mer, respectively. This expression can be rewritten as

$$x_n=n\{x_1\exp[(\mu_1^0-\mu_n^0)/kT]\}^n. \tag{A2}$$

If we assume that the methanol clusters are in a ''chain'' structure and that the free energy of bonding in each hydrogen bond is the same, the expression from the chemical potential with the monomer-monomer bonding free energy $-\alpha k_{\text{B}}T$ in the clusters is given by

$$n\mu_n^0=(n-1)\alpha k_{\text{B}}T, \tag{A3}$$

where α is a dimensionless parameter. In the present study, we treat the temperature dependence of the isochoric chemical shifts, then the Helmholtz free energy for hydrogen bond formation is equal to the negative monomer-monomer bond energy, i.e., $\Delta F=-\alpha k_{\text{B}}T$. Combining Eq. (A2) and (A3), the mole fractions of monomer (x_1), *n*-mer (x_n), and non-hydrogen-bonded proton ($x_{\text{N-HB}}$) are given, respectively, as,

$$x_1=\frac{1+2\mathrm{e}^{\alpha}-\sqrt{1+4\mathrm{e}^{\alpha}}}{2\mathrm{e}^{2\alpha}}, \tag{A4}$$

$$x_n=n(x_1\mathrm{e}^{\alpha})^n\mathrm{e}^{-\alpha}, \tag{A5}$$

$$x_{\text{N-HB}}=\frac{\sqrt{1+4\mathrm{e}^{\alpha}}-1}{2\mathrm{e}^{\alpha}}. \tag{A6}$$

[1] G. C. Pimentel and A. L. McClellan, *The Hydrogen Bond* (Freeman, San Francisco, 1960).
[2] R. W. Shaw, T. B. Brill, A. A. Clifford, C. A. Eckert, and E. U. Franck, C&E News **69**, 26 (1991).
[3] E. Kiran and J. F. Brennecke, *Supercritical Fluid Engineering Science* (American Chemical Society, Washington, D.C., 1993).
[4] N. Asahi and Y. Nakamura, Chem. Phys. Lett. **290**, 63 (1998).
[5] J. Jonas and J. A. Akai, J. Chem. Phys. **66**, 4946 (1977).
[6] N. Karger, T. Vardag, and H.-D. Lüdemann, J. Chem. Phys. **93**, 3437 (1990).
[7] J. G. Oldenziel and N. J. Trappeniers, Physica A **83**, 161 (1976).
[8] E. M. Shulman, D. W. Dwyer, and D. C. Doetschman, J. Phys. Chem. **94**, 7308 (1990).
[9] S. L. Wallen, B. J. Palmer, B. C. Garrett, and C. R. Yonker, J. Phys. Chem. **100**, 3959 (1996).
[10] M. M. Hoffmann and M. S. Conradi, J. Phys. Chem. B **102**, 263 (1998).
[11] M. Magini, G. Paschina, and G. Piccaluga, J. Chem. Phys. **77**, 2051 (1982).
[12] A. H. Narten and A. Habenschuss, J. Chem. Phys. **80**, 3387 (1984).
[13] D. G. Montague, I. P. Gibson, and J. C. Dore, Mol. Phys. **44**, 1355 (1981).
[14] T. W. Zerda, H. D. Thomas, M. Bradley, and J. Jonas, J. Chem. Phys. **86**, 3219 (1987).
[15] J. F. Mammone, S. K. Sharma, and M. Nicol, J. Phys. Chem. **84**, 3130 (1980).
[16] W. L. Jorgensen, J. Am. Chem. Soc. **103**, 341 (1981).
[17] W. L. Jorgensen and M. Ibrahim, J. Am. Chem. Soc. **104**, 373 (1982).
[18] W. L. Jorgensen, J. Phys. Chem. **90**, 1276 (1986).
[19] W. L. Jorgensen, J. Am. Chem. Soc. **102**, 543 (1980).
[20] M. Haughney, M. Ferrario, and I. R. McDonald, J. Phys. Chem. **91**, 4934 (1987).
[21] B. M. Pettitt and P. J. Rossky, J. Chem. Phys. **78**, 7296 (1983).
[22] J. Feeney and S. M. Walker, J. Chem. Soc. A **1966** 1148.
[23] M. Saunders and J. B. Hyne, J. Chem. Phys. **29**, 1319 (1958).
[24] J. C. Davis, K. S. Pitzer, and C. N. R. Rao, J. Phys. Chem. **64**, 1744 (1960).
[25] J. Israelachvili, *Intermolecular and Surface Forces*, 2nd ed. (Academic, San Diego, 1992).
[26] N. Asahi and Y. Nakamura, Ber. Bunsenges. Phys. Chem. **101**, 831 (1997).
[27] S. Shimokawa and E. Yamada, Rev. Sci. Instrum. **56**, 1220 (1985).
[28] P. O. Maurin, J. Dupuy-Philon, J. F. Jal, N. Asahi, T. Kamiyama, J. Kawamura, and Y. Nakamura, Ber. Bunsenges. Phys. Chem. **102**, 152 (1998).
[29] W. B. Kay and W. E. Donham, Chem. Eng. Sci. **4**, 1 (1955).
[30] R. J. B. Craven and K. M. de Reuck, Int. J. Thermophys. **7**, 541 (1986).
[31] H. Y. Carr and E. M. Purcell, Phys. Rev. **94**, 630 (1954).
[32] S. Meiboom and D. Gill, Rev. Sci. Instrum. **29**, 688 (1958).
[33] P. Stilbs, Prog. Nucl. Magn. Reson. Spectrosc. **19**, 1 (1987).

[34] R. E. Rathbun and A. L. Babb, J. Phys. Chem. **65**, 1072 (1961).
[35] F. H. A. Rummens and H. J. Bernstein, J. Chem. Phys. **43**, 2971 (1965).
[36] W. T. Raynes, A. D. Buckingham, H. J. Bernstein, J. Chem. Phys. **34**, 1084 (1961).
[37] A. A. Bothner-By, J. Mol. Spectrosc. **5**, 52 (1960).
[38] W. Smith and D. Fincham, CCP5 Program Library, Science and Research Council, Daresbury Laboratory, Warrington, U.K.
[39] R. L. Hurle, A. J. Easteal, and L. A. Woolf, J. Chem. Soc., Faraday Trans. 1 **81**, 769 (1985).
[40] J. O. Hirschfelder, C. F. Curtiss, and R. B. Bird, *Molecular Theory of Gases and Liquids* (Wiley, New York, 1966).
[41] L. Monchick and E. A. Mason, J. Chem. Phys. **35**, 1676 (1961).
[42] A. Rahman and F. H. Stillinger, J. Chem. Phys. **55**, 3336 (1971).
[43] A. G. Kalinichev and J. D. Bass, Chem. Phys. Lett. **231**, 301 (1994).
[44] P. Jedlovszky and R. Vallauri, Mol. Phys. **93**, 15 (1998).
[45] J. Martí, J. A. Padro, and E. Guardià, J. Chem. Phys. **105**, 639 (1996).
[46] J. C. Hindman, J. Chem. Phys. **44**, 4582 (1966).
[47] A. D. H. Clague, G. Govil, and H. J. Bernstein, Can. J. Chem. **47**, 625 (1969).